Electronic Supplementary Material (ESI) for New Journal of Chemistry.

Morphological adaptability through structural alterations in AIE active novel chemosensor with Al(III), Fe(III), and gas phase/aqueous phase TNP recognition ability

Pranabendu Das[b], Manik Das[a], Raju Biswas, Soumik Laha, Bidhan Chandra Samanta[c], [e] Tithi Maity[a]*

[a] Department of Chemistry, Prabhat Kumar College, Contai, Purba Medinipur, West Bengal, 721404, India

[b]Department of Chemistry, Indian Association for the Cultivation of Science, India

[c]Indian Institute of Chemical Biology, Jadavpur University, Kolkata, India

[c]Department of Chemistry, Mugberia Gangadhar Mahavidyalaya, Purba Medinipur, India

Email: titlipkc2008@gmail.com

Fig. No.	Index	Page

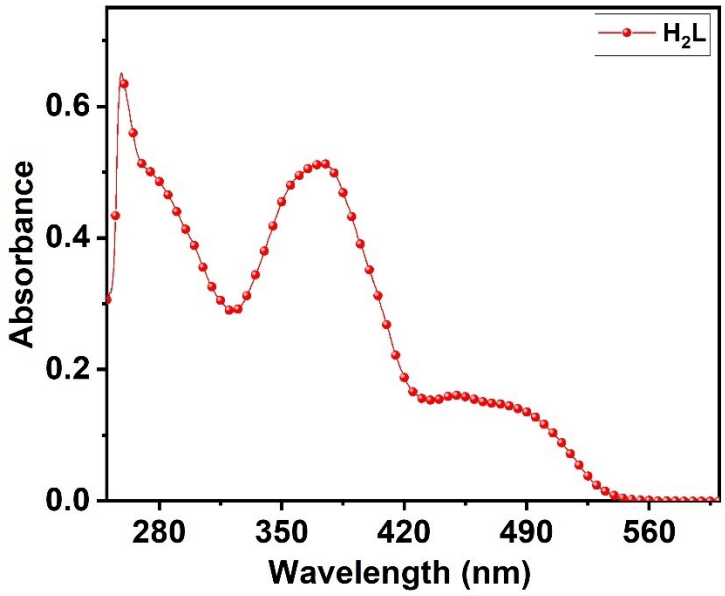

Fig. S1: Uv absorption spectra of the probe **H_2L**

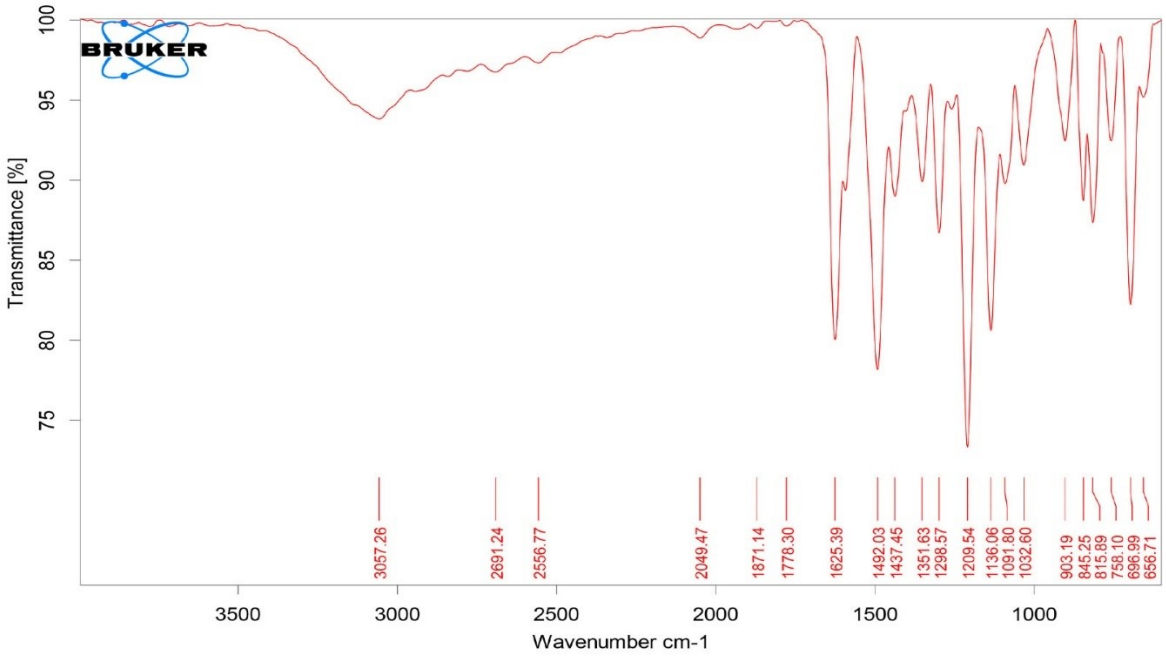

Fig. S2: FTIR spectra of **H_2L**

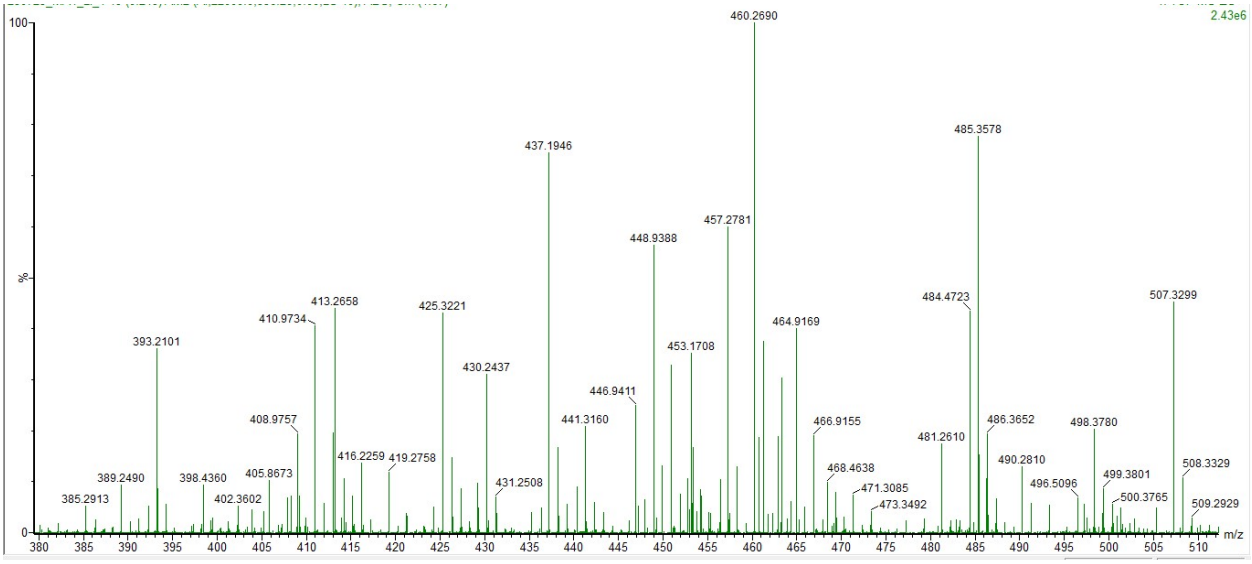

Fig. S3: Mass Spectra of $\mathbf{H_2L}$

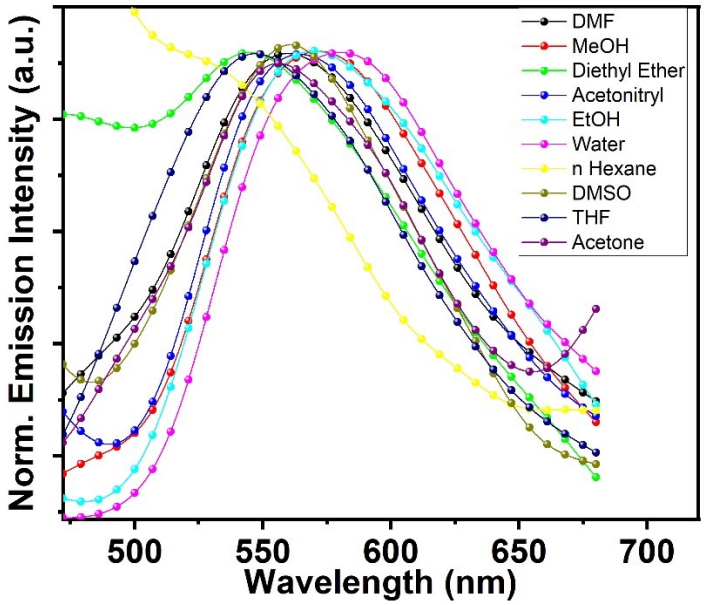

Fig. S4: Fluorescence spectra of $\mathbf{H_2L}$ in different solvents from non-polar to protic solvents to investigate the ESIPT process

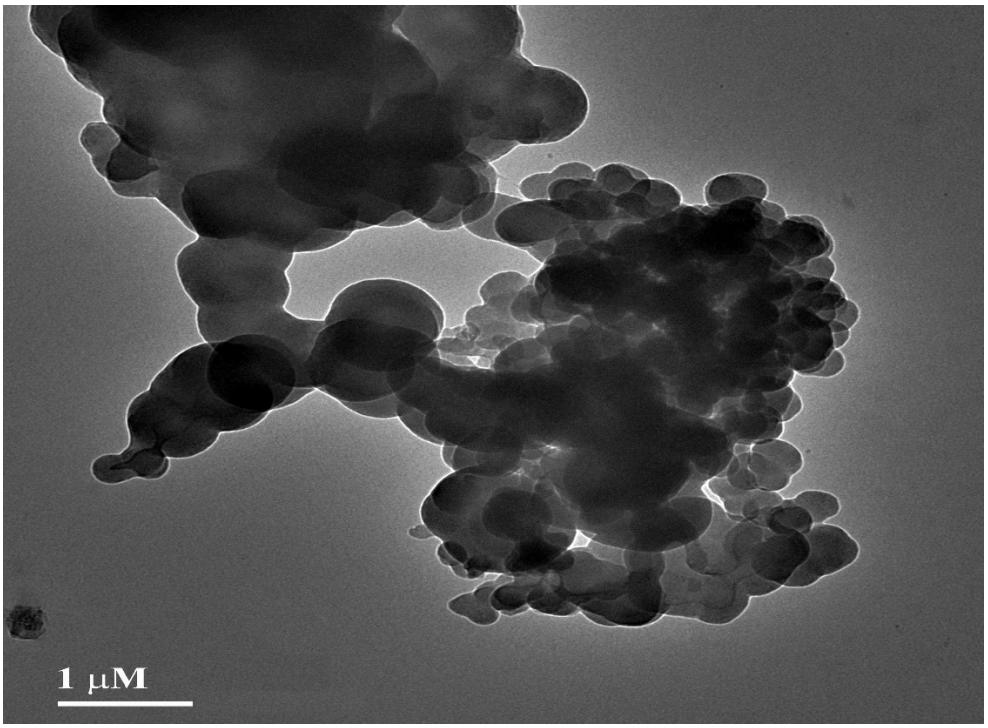

Fig. S5: TEM image of the probe in 7:3 DMSO-water mixture

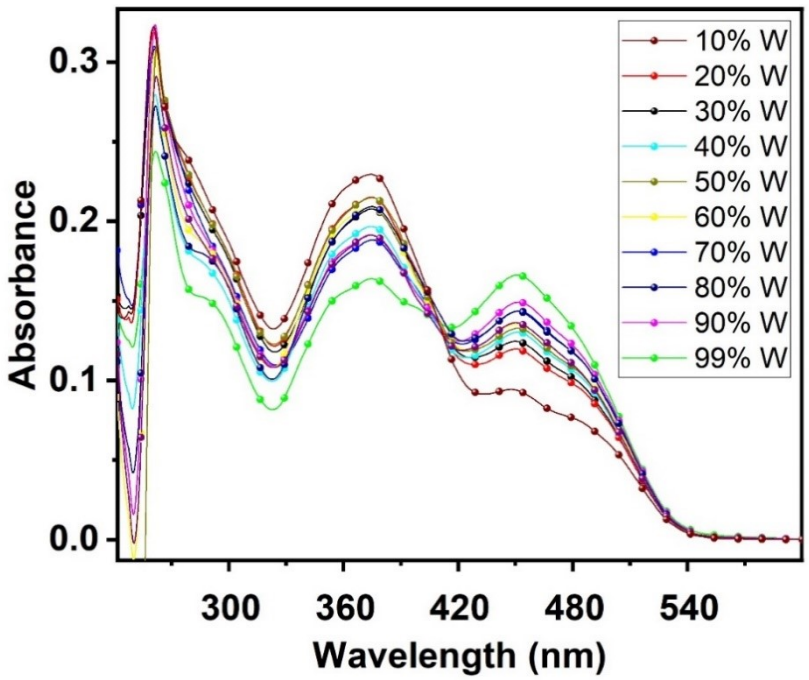

Fig. S6: Change of absorption spectra of $\mathbf{H_2L}$ (2×10^{-6} M) in different DMSO: H_2O mixtures.

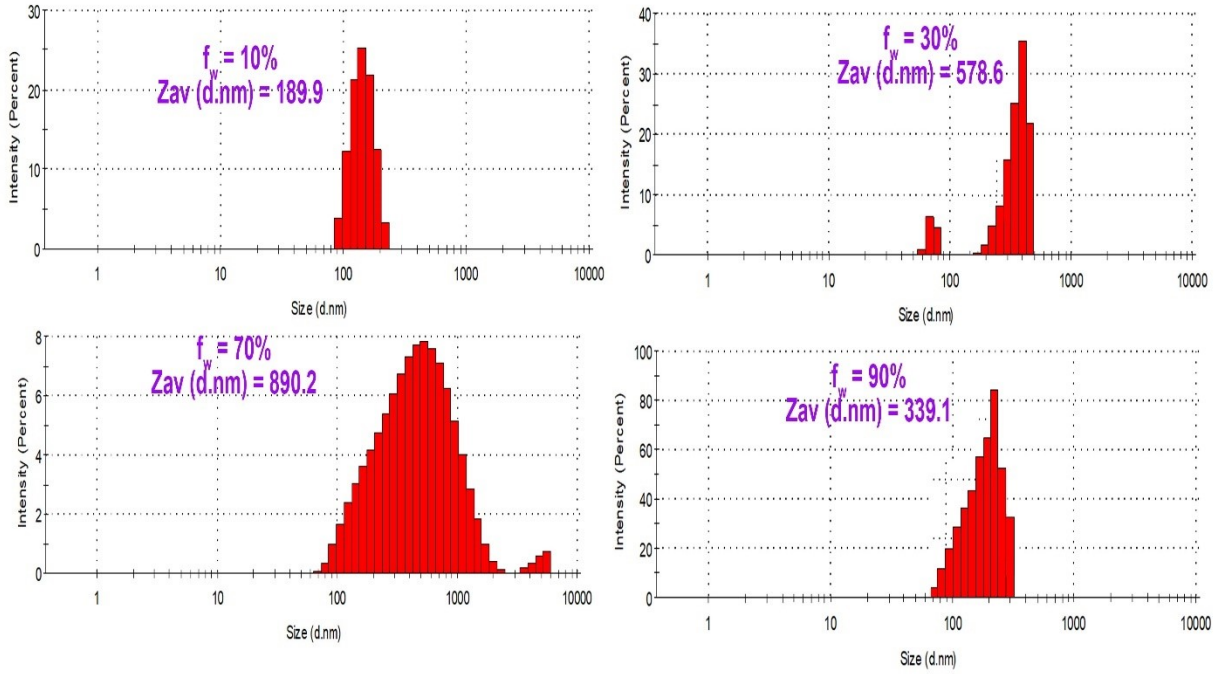

Fig. S7: DLS spectral analysis of $\mathbf{H_2L}$

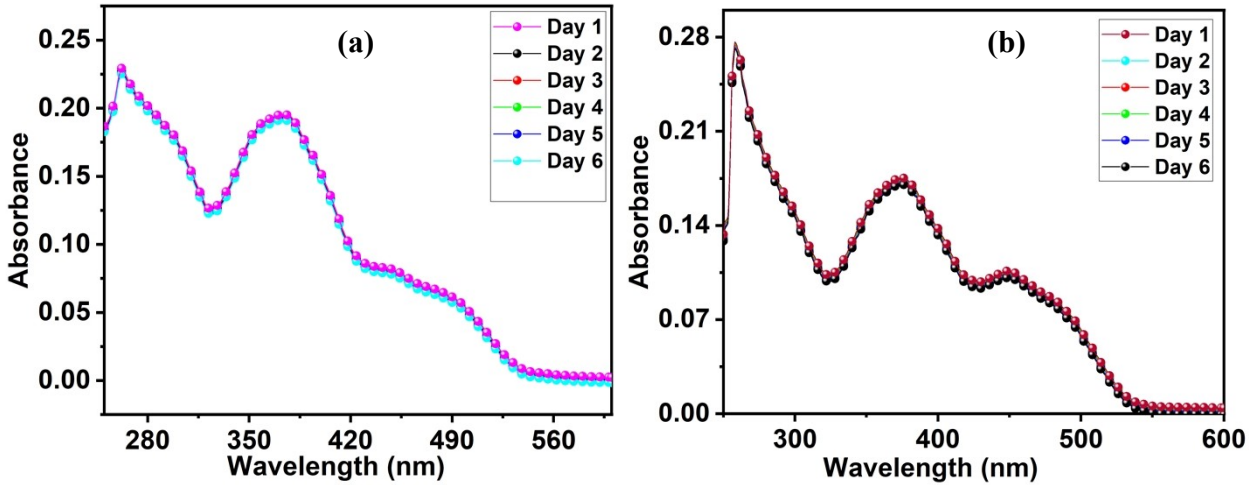

Fig. S8: Change of absorption spectra of $\mathbf{H_2L}$ as a function of time (a) in DMSO – H_2O (9:1 v/v) solvent (b) in AIEE solvent

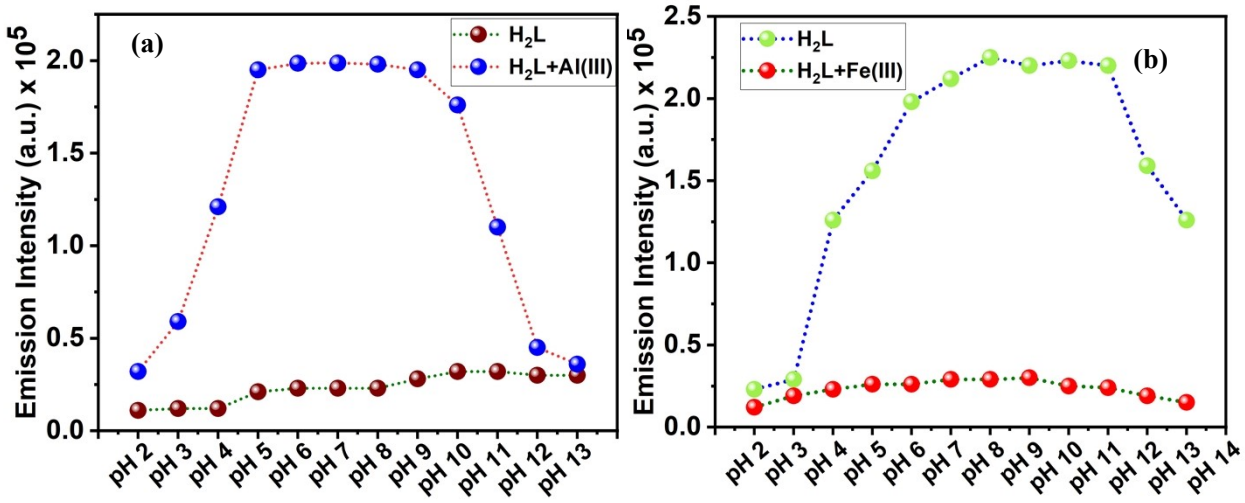

Fig. S9: (a) Change of Emission intensity of **H_2L** and **H_2L** – Al(III) adduct as a function of pH in DMSO – H_2O (9:1 v/v) HEPES buffer solution (b) Change of Emission intensity of **H_2L** and **H_2L** – Fe(III) adduct as a function of pH in AIEE solution

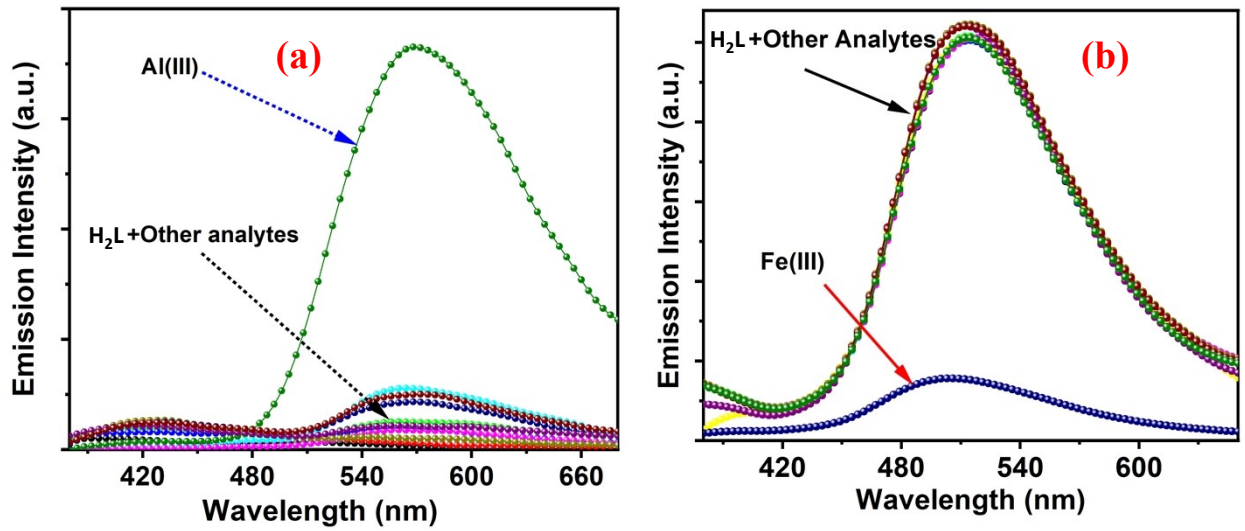

Fig. S10: Change of emission intensity of **H_2L** (3×10^{-6} M) in the presence of several cations (1×10^{-5} M) (a) in DMSO – H_2O (9:1 v/v) HEPES buffer media at pH 7.4 upon excitation at 370 nm (b) DMSO – H_2O (3:7 v/v) AIEE media upon excitation at 375 nm

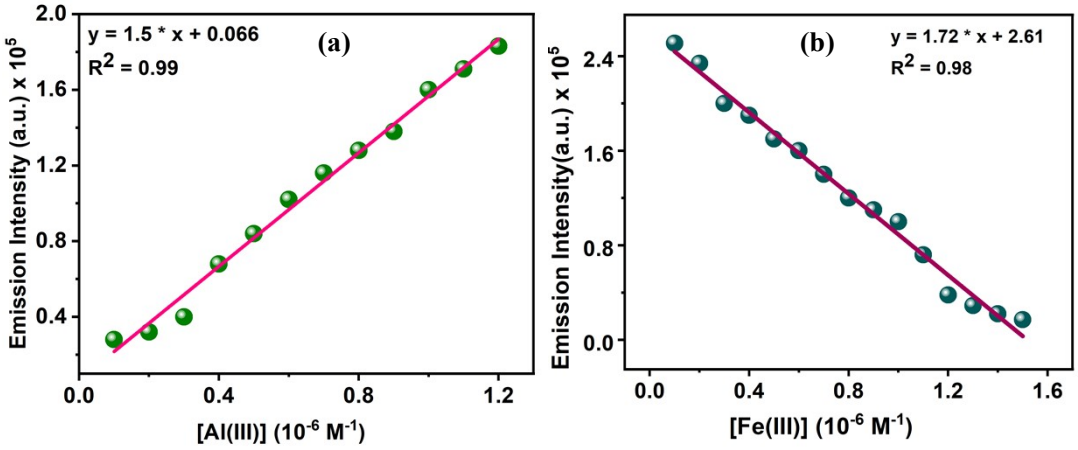

Fig. S11: Plot of Emission intensity vs concentration of metal ion to determine the LOD value for (a) $\mathbf{H_2L}$ – Al(III) and (b) $\mathbf{H_2L}$ – Fe(III) adducts

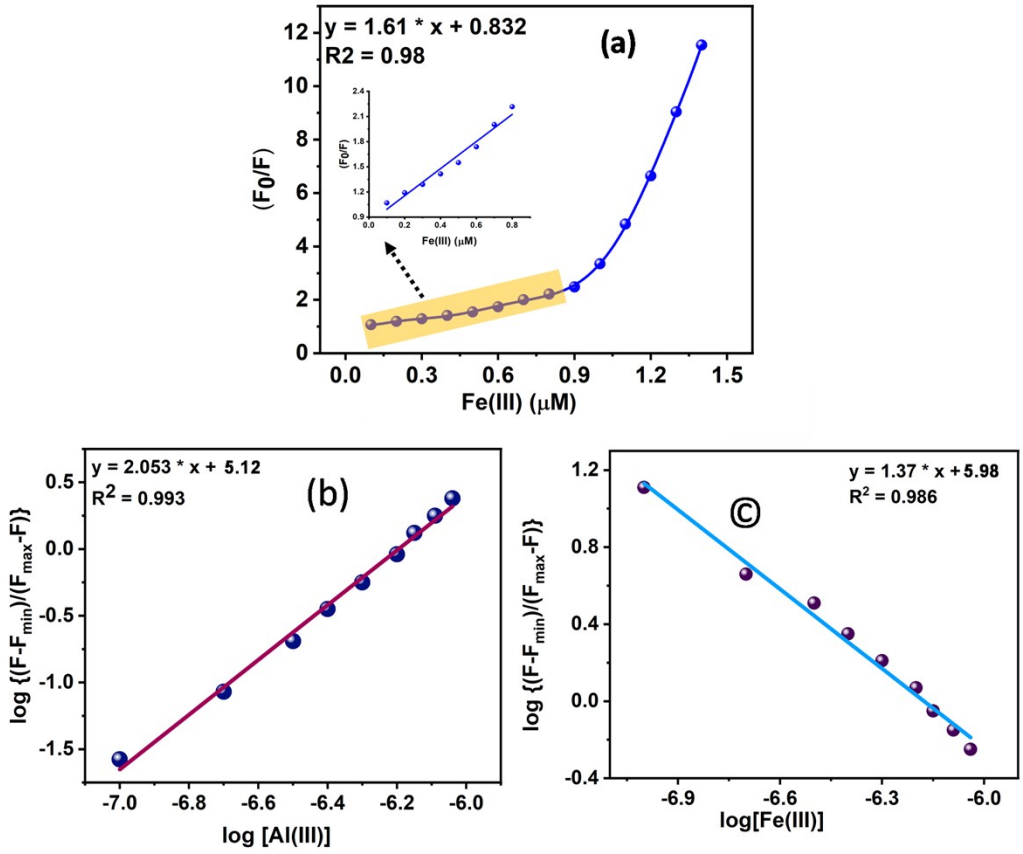

Fig. S12: (a) Stern-Volmer plot in determining quenching constant after the introduction of Fe(III) to $\mathbf{H_2L}$. Binding constant determination plot for (b) $\mathbf{H_2L}$ – Al(III) adduct and (c) $\mathbf{H_2L}$ – Fe(III) adduct from fluorescence spectral data.

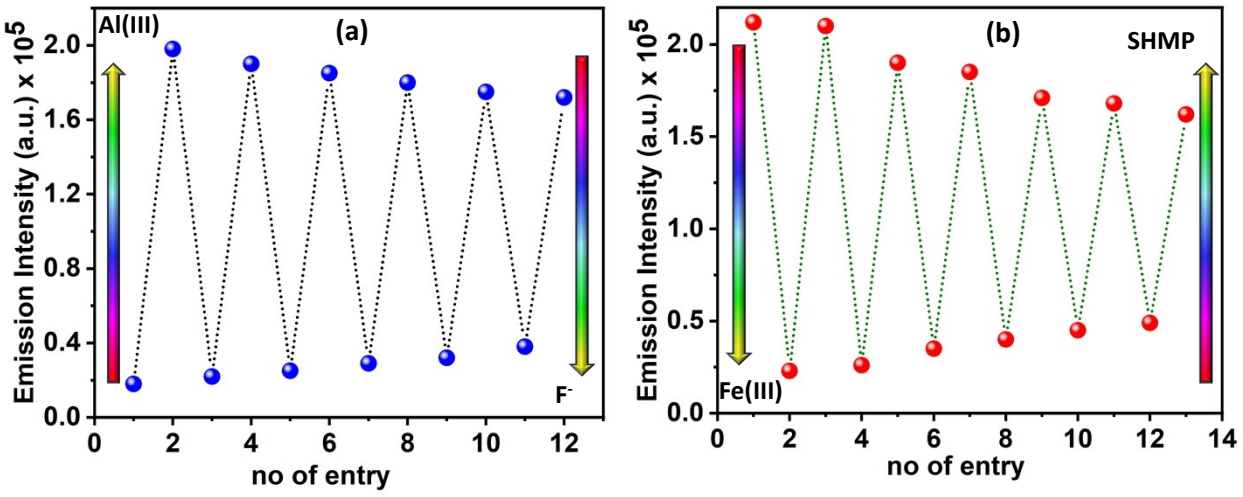

Fig. S13: reversibility experiment of **H_2L** (a) by alternative addition of Al(III) and NaF in DMSO – H_2O (9:1 v/v) HEPES buffer media (b) by alternative addition of Fe(III) and SHMP in AIEE solvent.

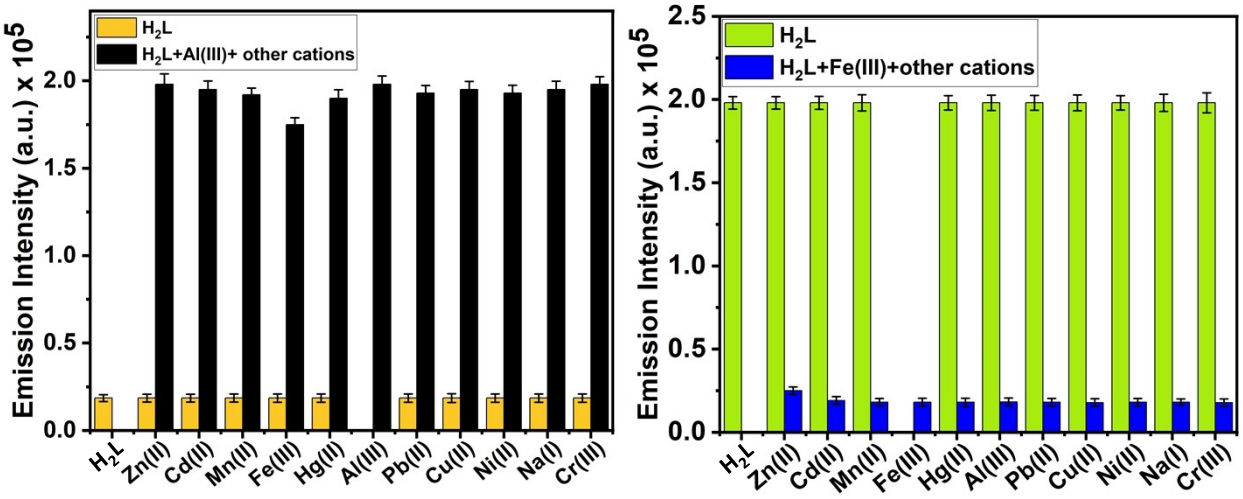

Fig. S14: Change of Emission intensity of **H_2L** – Al(III)/Fe(III) adduct in the presence of several competitive cations in (a) DMSO – H_2O (9:1 v/v) HEPES buffer solution (b) AIEE solvent

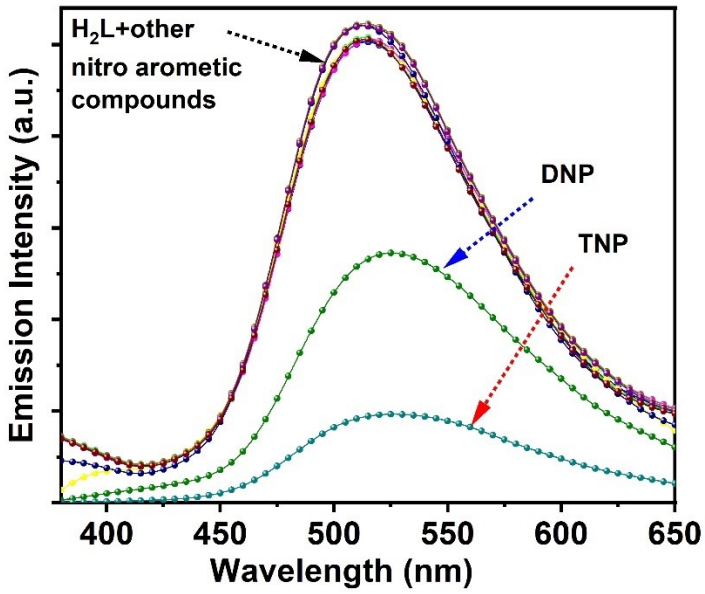

Fig. S15: Change of fluorescence spectra of $\mathbf{H_2L}$ after separative addition of different NACs in AIEE solvent.

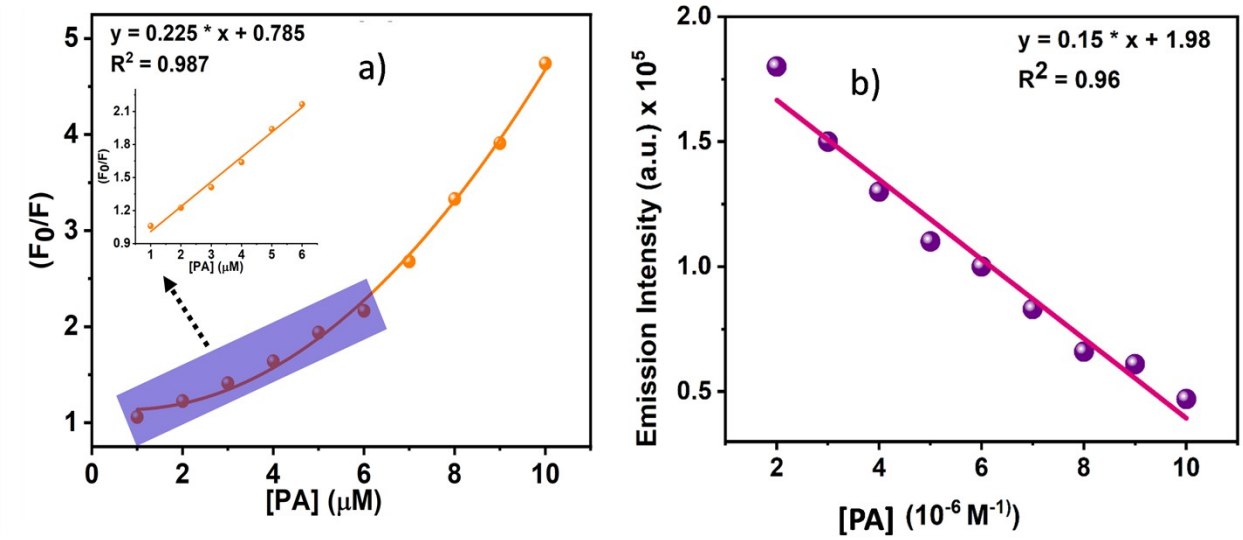

Fig. S16: a) Stern-Volmer plot in determining quenching constant after the introduction of picric acid to $\mathbf{H_2L}$. b)LOD determination plot for TNP from the linear fitting plot of Emission intensity vs concentration of TNP

Table 1: Sensing parameters of several literature reported Schiff base probe with cations or TNP sensing ability

Sl No	Probe	Ion detection	Solvent (v/v)	LOD (M)	Sensing Technique	Application	References
01	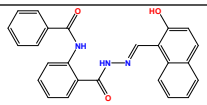	Al(III)	MeOH -H_2O (9:1)	1.68×10^{-9}	Fluorometric	Paper Strip, Cell imaging	1
02	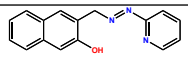	Al(III)	MeOH	1.81×10^{-8}	Fluorometric	No	2
03	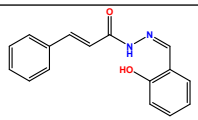	Zn(II), Al(III)	MeOH	3.15×10^{-7} 2.98×10^{-7}	Fluorometric	No	3
04	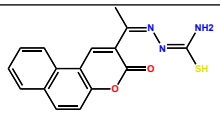	Fe(III)	H_2O	7.6×10^{-5}	Fluorometric	Real water	4
05	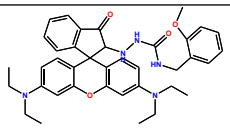	Fe(III)	MeOH -H_2O (1:1)	1.28×10^{-8}	Fluorometric	Cell Imaging, Real water	5
06	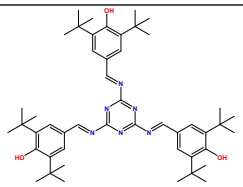	Al(III), Fe(II)	H_2O	3.98×10^{-5} 1.85×10^{-5}	Colourimetric And Fluorometric both	No	6
07	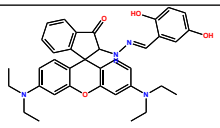	Al(III), Fe(III)	MeOH -H_2O (1:1)	1.1×10^{-8} 1.9×10^{-8}	Colourimetric Fluorometric	Paper strip	7

08	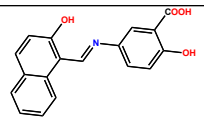	Cu(II), Cr(III) Al(III), Fe(III)	DMF-H_2O (1:1)	4.65×10^{-7} 3.37×10^{-7} 3.58×10^{-7} 4.89×10^{-7}	Colourimetric Colourimetric Fluorometric Fluorometric	No	8
09	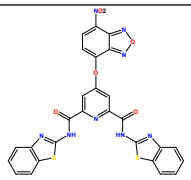	Al(III) Fe(III)	THF, MeOH, H_2O	4.38×10^{-9} 6.74×10^{-7}	Colourimetric Fluorometric both	Logic gate	9
10	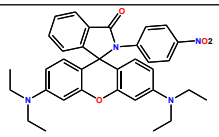	Al(III)	MeCN-H_2O (2:8)	3.0×10^{-5}	Colourimetric Fluorometric both	Cell imaging	10
11	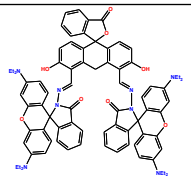	Al(III), Cr(III) Fe(III), Cu(II)	MeOH-H_2O (9:1)	2.27×10^{-6} 1.29×10^{-6} 1.75×10^{-6} 1.21×10^{-6}	Fluorometric	Cell imaging Paper strip	11
12	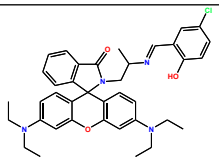	Hg(II), TNP (not in vapour state)	EtOH-H_2O (2:8)	2.43×10^{-8} 8.37×10^{-8}	Fluorometric	Cell imaging	12
13	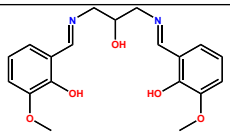	Al(III), TNP (not in vapour state)	H_2O	1.13×10^{-8} 2.01×10^{-8}	Fluorometric	Cell imaging	13

14	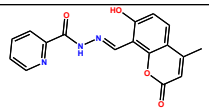	Al(III), TNP(not in vapour state)	DMSO-H_2O (1:9)	6.99×10^{-9} 1.67×10^{-6}	Fluorometric	Logic gate	14
15	Ni – MOF	TNP (not in vapour state)	MeCN, Gas	2.9×10^{-5}	Fluorometric	N_2 Adsorption	15
16	Dy – MOF	TNP(not in vapour state)	H_2O, Gas	1.25×10^{-5}	Fluorometric		16
17	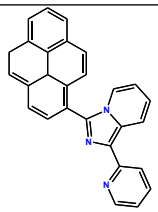	TNP(not in vapour state)	DMF	6.9×10^{-8}	Fluorometric	Portable device	17
18	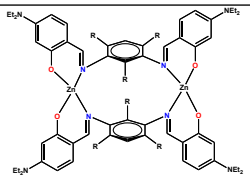	TNP(not in vapour state)	MeCN	5.5×10^{-9}	Fluorometric	Paper Strip	18
19	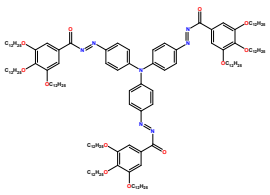	TNP(not in vapour state)	Gas	9.8×10^{-10}	Colourimetric Fluorometric both	Paper strip	19
20	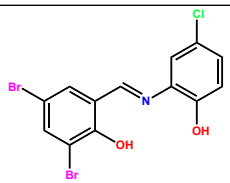	Al(III), Fe(II), TNP(not in vapour state)	DMSO-H_2O, Gas	6.02×10^{-9}, 7.5×10^{-9}, 6.0 × 10^{-8}	Colourimetric Fluorometric both	Al(III) detection and quantification	Present Work

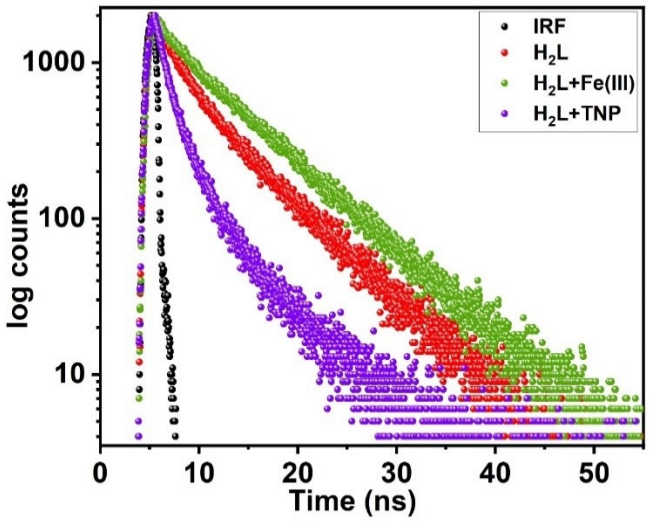

Fig. S17: Time-resolved fluorescence decay of probe **H_2L** in the presence and absence of Fe (III) and TNP

Table S2: Different parameter values during lifetime experiments of **H_2L** in the presence and absence of Fe(III) and TNP

Sample	τ_1	τ_2	α_1	α_2	χ^2	τ_{av}
H_2L (10 μM)	1.35	7.62	0.318	0.681	1.146	5.618
H_2L (10 μM) + Fe(III) (10 μM)	1.95	7.04	0.586	0.414	1.08	4.05
H_2L (10 μM) + TNP	1.142	4.64	0.424	0.575	1.154	3.15

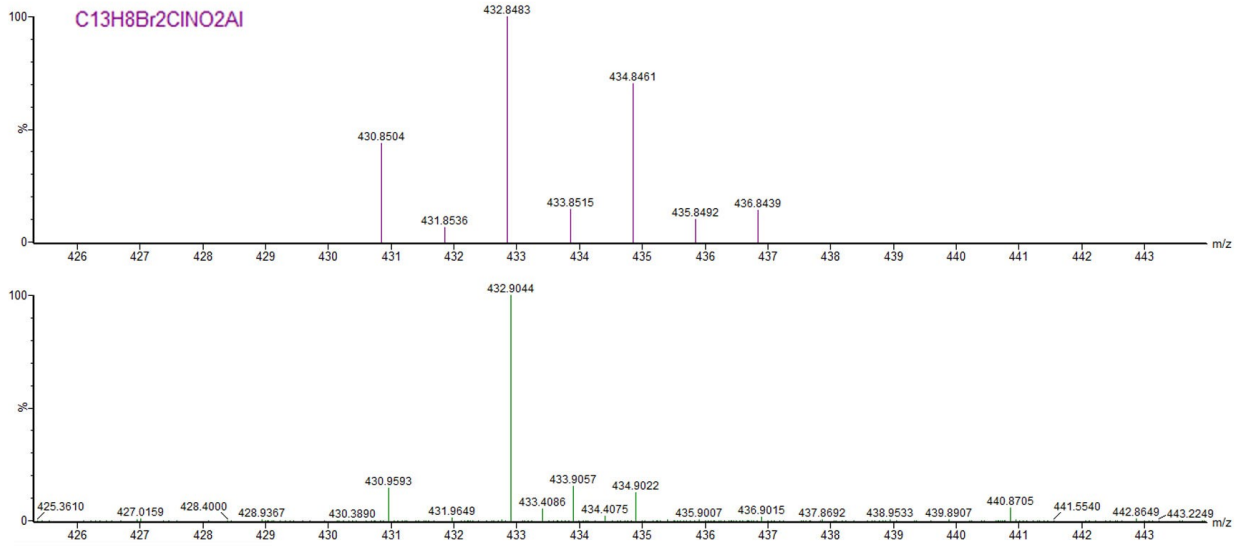

Fig. S18: MASS spectra of $\mathbf{H_2L}$ – Al(III) adduct

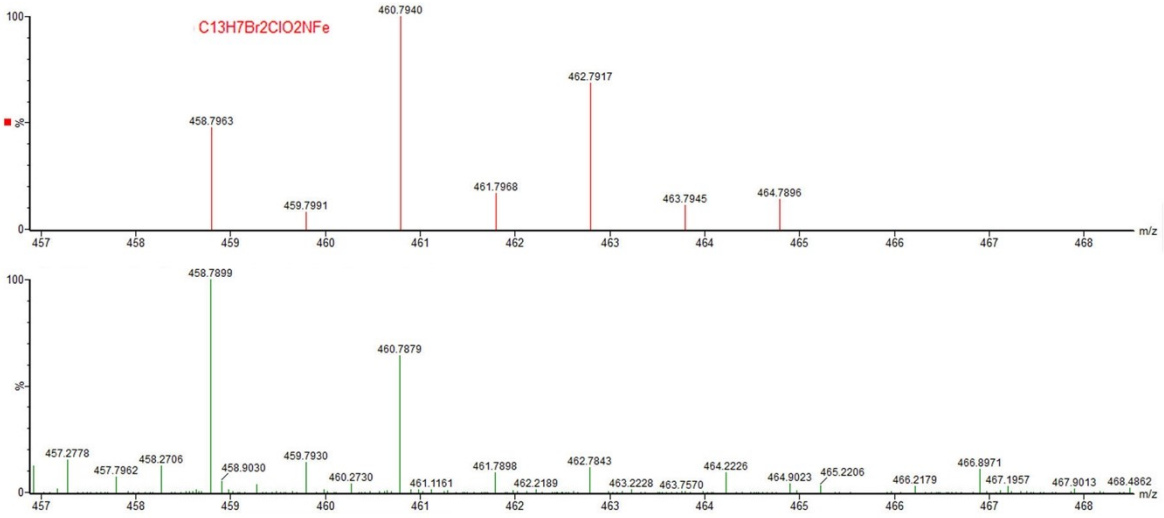

Fig. S19: MASS spectra of $\mathbf{H_2L}$ – Fe(III) adduct

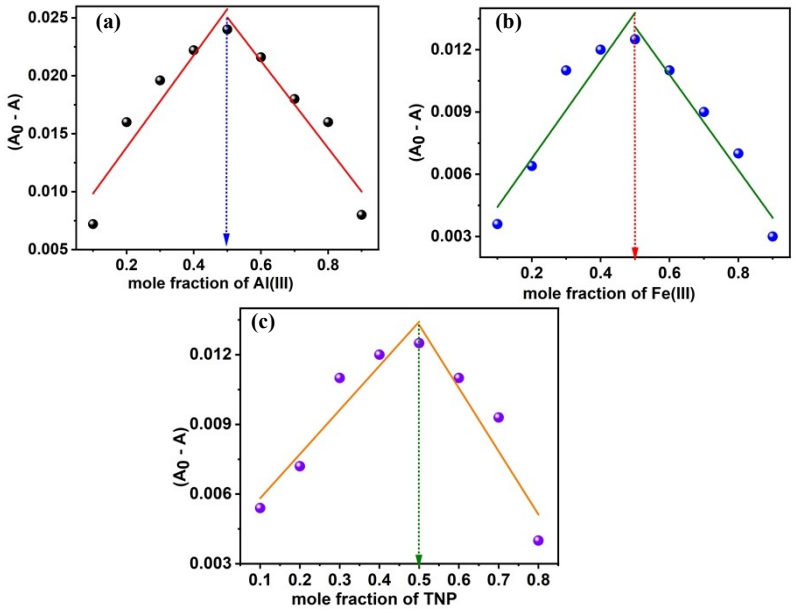

Fig. S20: Job's plot for the determination of 1:1 stoichiometry complexation of **H_2L** and (a) Al(III) (b) Fe(III) and (c) TNP

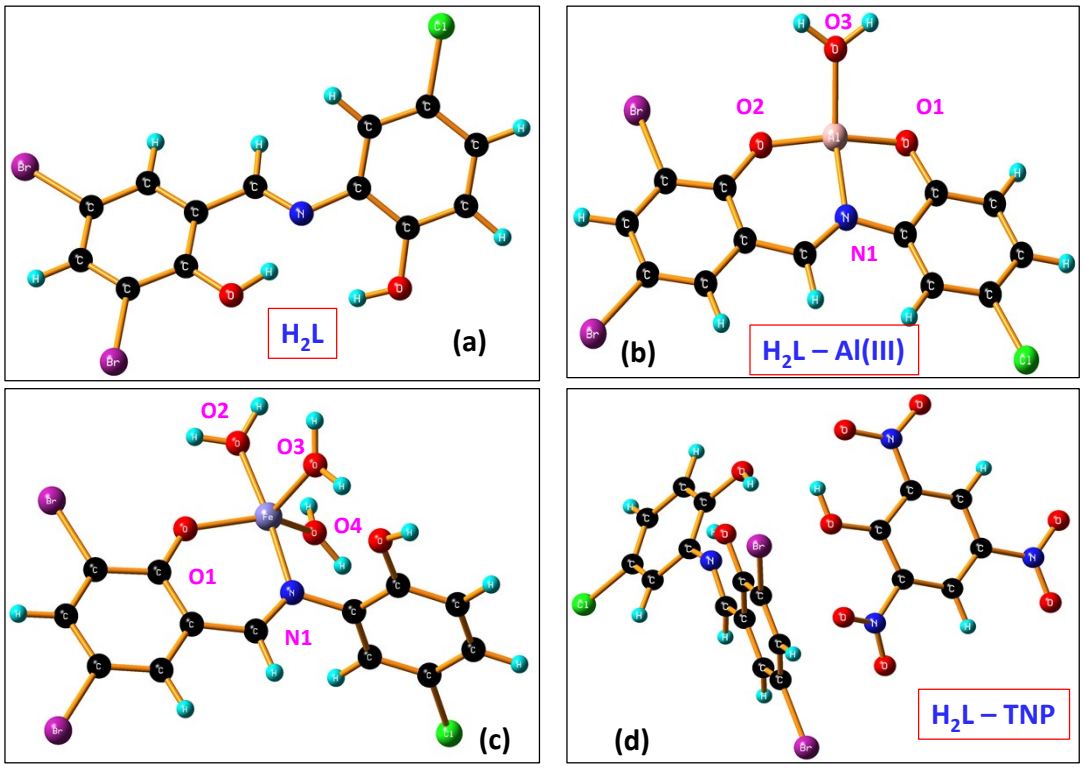

Fig. S21: DFT optimized electronic structure of (a) **H_2L** (b) **H_2L**- Al(III) Complex (c) **H_2L**-Fe(III) Complex (d) **H_2L**- TNP adduct

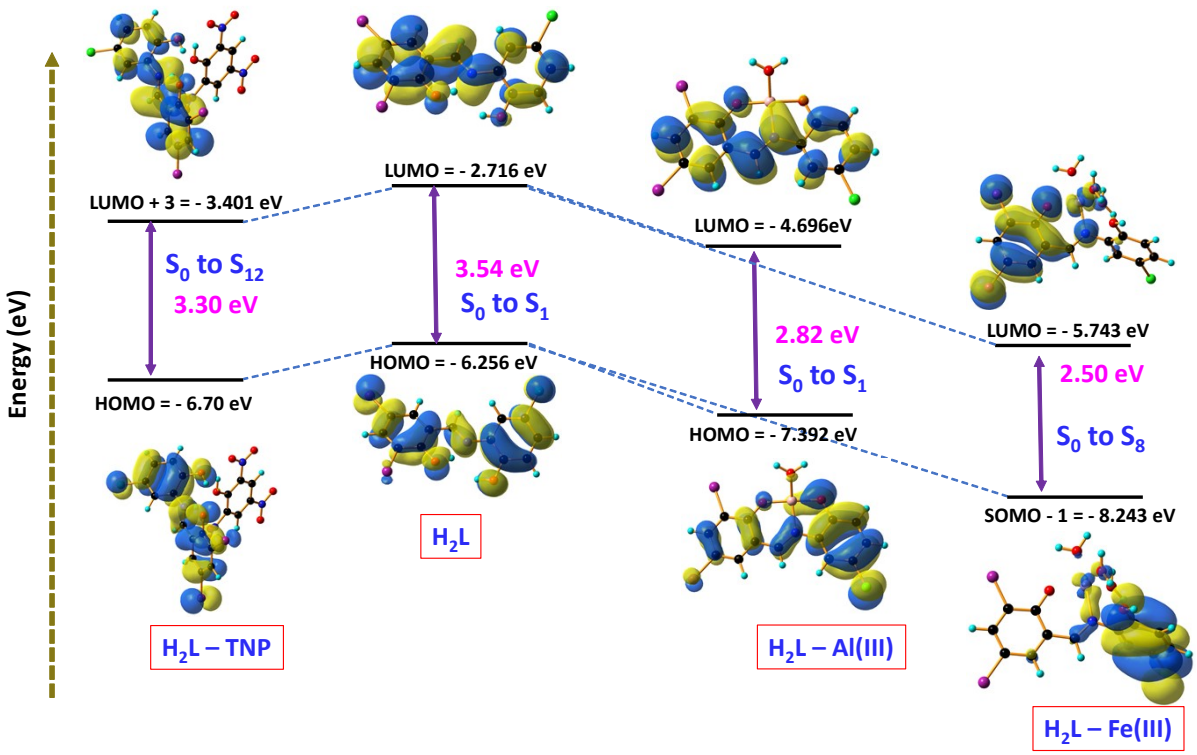

Fig. S22: HOMO-LUMO energy gap for **H_2L**, **H_2L**-Al(III), **H_2L**-Fe(III), **H_2L**-TNP

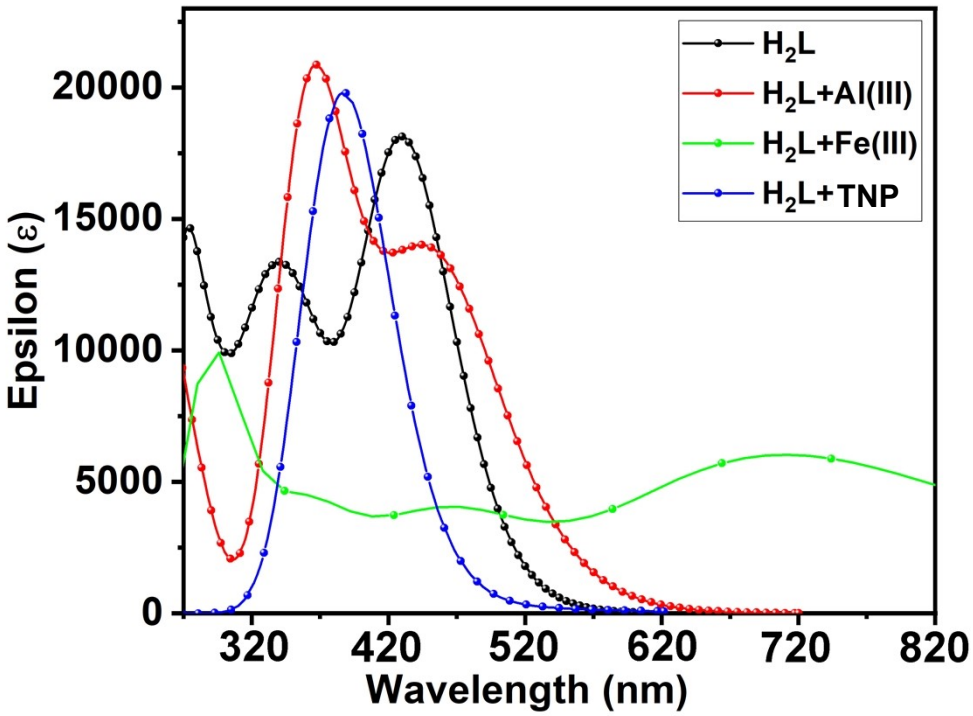

Fig. S23: DFT optimized electronic spectra of the Probe and the probe analyte complexes

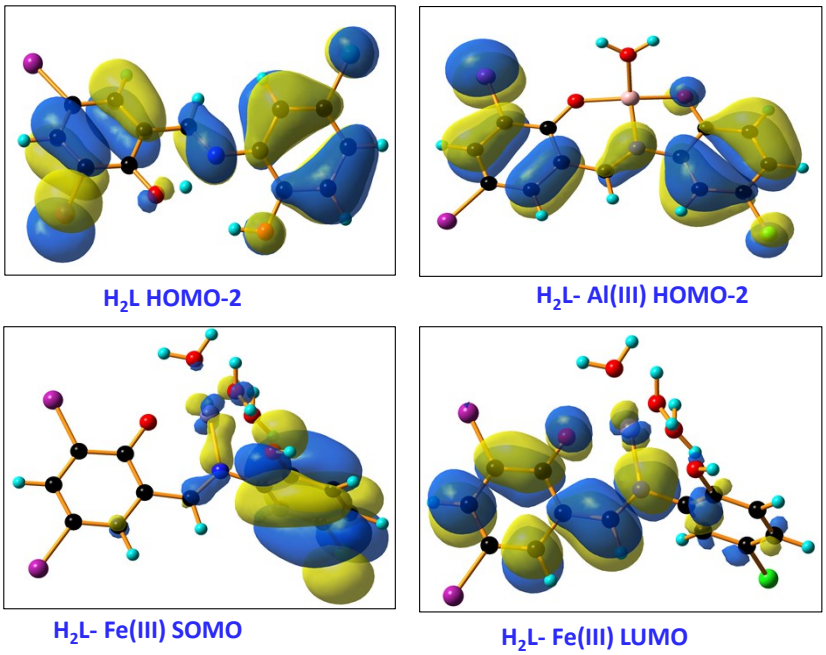

Fig. S24: Frontier Molecular Orbital images of the probe **H_2L** and the Probe analyte complexes

Table S3: Selected Bond distance and Bond angles of **H_2L**, **H_2L**-Al(III) complex, **H_2L**-Fe(III) complex and **H_2L**-TNP adduct in the ground state geometry

compounds	Bond distance(Å)		Bond angle (degree)	
H_2L-Al(III) complex (Distorted Tetrahedral)	Al-O1(L)	1.785	O1- Al -N1	88.30
	Al-O2(L)	1.757	O1- Al -O2	154.93
	Al-N1	1.932	O3- Al -N1	138.32
	Al – O3(W)	1.854	O3- Al -O2	96.55
			O3- Al -O1	97.18
			O2- Al -N1	95.20
H_2L-Fe(III) complex (Distorted Square pyramidal)	Fe-N1	1.966	N1- Fe -O1	92.22
	Fe-O1	1.940	N1- Fe -O2	174.95
	Fe-O2	1.989	N1- Fe -O3	93.45
	Fe-O3	1.984	N1- Fe -O4	94.82
	Fe -O4	2.00	O1- Fe -O2	83.63
			O1- Fe -O3	116.43
			O1- Fe -O4	132.00
			O2- Fe -O3	90.97
			O2- Fe -O4	85.87
			O3- Fe -O4	110.43

H_2L-TNP adduct	O1(L)--H(O)	2.10		

Table S4: Molecular Orbital, involved the Major Electronic Transitions with Osc. Strength of **H_2L**, **H_2L** – Al(III) Complex, **H_2L** – Fe(III) Complex and **H_2L**-TNP adduct

Compounds	Wavelength(nm)	Osc. Strength	Electronic Transition
H_2L	340.25	0.2127	H-2(A) – L(A)
	420.18	0.4191	H(A) – L(A)
H_2L-Al(III) complex	360.08	0.2783	H(A) – L(A)
	445.48	0.4987	H-2(A) – L(A)
H_2L-Fe(III) complex	368.29	0.0593	S-1(A) – L(A)
	470.34	0.0518	S(A) – L+1(A)
	720.39	0.1095	S-9(A) – L(A)
H_2L-TNP adduct	385.13	0.5141	H(A) – L+3(A)

Table S5: Measured amount of Al(III) concentration in market-available drug samples along with a comparison with HPLC method

Sample Name	**Conc. Of H_2L (μM)**	**Amount of sample solution taken (ul)**	**Measured Conc. Of Al(III) (μM)**	**Average Conc. Of Al(III) (μM)**	**HPLC Method (μM)**
Gelusil	1	100	0.942	0.942	0.90
	1	100	0.941		
	1	100	0.942		
Diagene	1	100	0.789	0.794	0.76
	1	100	0.798		
	1	100	0.795		

Diovol	1	100	0.536	0.535	0.51
	1	100	0.536		
	1	100	0.534		
Disprin	1	100	0.412	0.418	0.41
	1	100	0.420		
	1	100	0.423		
Nexpro rd	1	100	0.205	0.207	0.22
	1	100	0.208		
	1	100	0.209		
Telma	1	100	0.155	0.155	0.17
	1	100	0.153		
	1	100	0.157		

References

1. A Bhattacharyya, S. C. Makhal, and N. Guchhait, *ACS Omega,* 2018, **3**, 11838−11846.
2. V. K. Gupta, S. K. Shoora, L. K. Kumawat, and A. K. Jain, *Sensors Actuators, B Chem.* 2015, **209**, 15–24.
3. R. Patra, and K. K Rajak, *ChemistrySelect,* 2020, **5**, 9477 – 9485.
4. G. M. Khairy, A. S. Amin, S. M. N. Moalla, A. Medhat , and Nader Hassan, *RSC Adv.***,** 2022,**12**, 27679-27686.
5. Z. Wu, Z. Xu, H. Tan, X. Li, J. Yan, C. Dong and L. Zhang, *Spectrochim. Acta, Part A*, 2019, **213** , 167 —175.
6. U. D. Kamaci, M. Kamaci, and Aysegul Peksel, *Spectrochimica Acta Part A: Molecular and Biomolecular Spectroscopy,* 2021, **254**, 119650.

7. V. K. Gupta N. Mergu, and L. K. Kumawat, *Sensors and Actuators B,* 2016, **223**, 101 – 113.
8. M, Zhang, L. Gong, C. Sun, W. Li, Z. Chang, and D. Qi, *Spectrochimica Acta Part A: Molecular and Biomolecular Spectroscopy,* 2019, **214**, 07 – 13.
9. R. Gupta, S. S. Malak, V. Kumar and P. Kumar, *New J. Chem*., 2020, **44**, 13285-13294.
10. S. Das, U. Mukherjee, S. Pal, S. Maitra and P. Sahoo, *Org. Biomol. Chem*., 2019, **17**, 5230-5233.
11. B. Das, A. Ghosh, D. P. Dorairaj, M. Dolai, R. Karvembu, S. Mabhai, H. Im, S. Dey, and A. Misra, Journal of Molecular Liquids, 2022, 354, 118824.
12. S. Das, M. Das, U. K. Das, B. C. Samanta, A. Bag, A. Patra, N. Bhattacharya, T. Maity, *Dyes and Pigments,* 2024, 222, 111884.
13. B. Naskar, A. Bauzá, A. Frontera, D. K. Maiti, C. D. Mukhopadhyay, and S. Goswami, *Dalton Trans.* 2018, **47**, 15907-15916.
14. R. Purkait, A. Dey, S. Dey, P. P. Ray and C. Sinha, *New J. Chem*., 2019, **43**, 14979-14990.
15. S, Chongdar, U. Mondal, T. Chakraborty, P. Banerjee, and A. Bhaumik, ACS Appl. Mater. Interfaces 2023, **15**, 11, 14575–14586.
16. S. Mukherjee, S. Ganguly, A. Chakraborty, A. Mandal, and D. Das, ACS Sustainable Chem. Eng. 2019, **7**, 1, 819–830.
17. A. Kathiravan, A. Gowri, T. Khamrang, M. D. Kumar, N. Dhenadhayalan, K. C. Lin, M. Velusamy, and M. Jaccob, Anal. Chem. 2019, **91**, 20, 13244–13250.
18. A. Kumar, A. Kumar and S. Pandey, *Dalton Trans.,* 2016, **45**, 8475-8484.
19. A. K. Nandi, S. Mondal, P. Bairi, and Sujoy Das, *Chemistry – A European Journal*, 2018, **24,** 5591 – 5600.